GEOLOGICA CARPATHICA, APRIL 2013, 64, 2, 153–163 doi: 10.2478/geoca-2013-0011

Correlation between geology and concentration-volume fractal models: significance for Cu and Mo mineralized zones separation in the Kahang porphyry deposit (Central Iran)

AMIR BIJAN YASREBI[1]✉, PEYMAN AFZAL[1,2], ANDY WETHERELT[1], PATRICK FOSTER[1] and REZA ESFAHANIPOUR[3]

[1]Camborne School of Mines, University of Exeter, Cornwall Campus, TR10 9EZ Penryn, United Kingdom;
✉aby203@exeter.ac.uk
[2]Department of Mining Engineering, South Tehran branch, Islamic Azad University, Tehran, Iran
[3]National Iranian Copper Industries Co. (NICICO)

(Manuscript received May 15, 2012; accepted in revised form October 19, 2012)

Abstract: This study identifies the major mineralized zones including supergene enrichment and hypogene enrichment in the Kahang Cu-Mo porphyry deposit which is located in Central Iran based on subsurface data and utilization of the concentration-volume (C-V) fractal model. Additionally, a correlation between results achieved from a C-V fractal model and geological models consisting of zonation, mineralography and alteration have been conducted in order to have an accurate recognition and modification of the main mineralized zones. Log-log plots indicate five geochemical populations for Cu and Mo in the deposit which means that mineralization commences with 0.075 % and 13 ppm for Cu and Mo (as the first thresholds) respectively. The main mineralization began for Cu≥0.42 % and Mo≥100 ppm and also enriched mineralization containing Cu≥1.8 % and Mo≥645 ppm which is located in the central part of the deposit. According to the C-V model, the main Cu-Mo mineralized zones occur in the hypogene zone, especially in the central, NW and NE parts of the Kahang deposit. The supergene enrichment zone derived via the C-V model is smaller than that in the geological model and is located in the central and eastern parts of the deposit. Results analysed by the C-V fractal model certify that the interpreted zones based on the fractal model are accurate. To certify this, a logratio matrix has been employed to validate the C-V fractal model for the Cu and Mo main mineralized zones.

Key words: Iran, Kahang, mineralized zones, copper-molybdenum porphyry deposit, concentration-volume (C-V) fractal model.

Introduction

Identification of mineralized zones plays a significant role in exploration of porphyry deposits. The conventional geological methods to identify mineralized zones in porphyry deposits are mineralogical and petrographical studies (Schwartz 1947; Lowell 1968; Lowell & Guilbert 1970; Beane 1982; Cox & Singer 1986; Sillitoe 1997; Melfos et al. 2002; Berger et al. 2008). Fluid inclusion and sulphur isotope studies (e.g. Roedder 1971; Nash 1976; Ulrich et al. 2001; Wilson et al. 2007; Asghari & Hezarkhani 2008) are other methods which have been employed. However, in all of the models, ore grades were not considered to distinguish different mineralized zones and it is believed that ore grades vary in relation to changes in the geological properties such as mineralogy, lithology and alterations. Various geological interpretations can define different boundaries of mineralized zones in porphyry deposits which potentially result in the ore element grade distribution (Afzal et al. 2011).

In recent years, models based on fractal geometry proposed by Mandelbrot (1983) have been widely applied in different branches of earth sciences since various geochemical processes can be characterized by changes in fractal dimensions resulting from analysis of relevant geochemical data (e.g. Turcotte 1986; Lucido et al. 1991; Agterberg et al. 1993; Cheng et al. 1994; Sim et al. 1999; Goncalves et al. 2001; Shen & Zhao 2002; Li et al. 2003; Lima et al. 2003; Ortega et al. 2006; Ali et al. 2007; Carranza 2009; Zuo et al. 2009; Afzal et al. 2010; Wang et al. 2011; Zuo 2011).

Fractal analysis is able to indicate and correspondingly justify the differences within mineralization, alteration, lithology and zonation of ore deposits especially in hydrothermal occurrences such as porphyry Cu deposits (Goncalves et al. 2001; Cheng 2007; Carranza 2008; Carranza et al. 2009; Cheng & Agterberg 2009; Afzal et al. 2011, 2012). However, proper knowledge of the geological and geochemical aspects of a deposit is important in order to identify characteristics of geochemical populations on the basis of fractal analysis (Cheng 1999; Sim et al. 1999; Goncalves et al. 2001; Li et al. 2003; Carranza 2009; Carranza & Sadeghi 2010). In other words, variations of fractal dimensions in geochemical data can present applicable criteria to recognize mineralized zones and barren host rocks within a study area.

The aim of this study is to use a concentration-volume (C-V) fractal model to delineate Cu and Mo mineralized zones in the Kahang porphyry deposit of Central Iran, and to correlate and validate the results with geological models consisting of zonation and alteration by logratio matrix as proposed by Carranza (2011).

Significance and merits of fractal approach and dimensions

Euclidian geometry classifies geometrical features with an integer dimension say 1D, 2D, 3D, etc. However, there are many spatial objects, whose dimensions cannot be mathematically defined by integers but by real numbers or fractions called fractals which describe complexity in data distribution by estimation of their fractal dimensions. Different geochemical processes can be explained on the basis of variations in fractal dimensions obtained from analysis of relevant geochemical data. Fractals are determined by a scaling law that relates two variables: the scale factor (frequency) and the object being measured (size). Fractal dimensions in geological and geochemical processes correspond to differences in physical characteristics such as lithology, vein density or orientation, fluid phase, alteration phenomena, structural feature or dominant mineralogy (Takayasu 1990; Lauwerier 1991; Sim et al. 1999; Ortega et al. 2006). Conventional methods based upon surface geological studies and analysis of cores from boreholes in order to separate the mineralized zones do not have the high accuracy particularly in porphyry deposits. The fractal geometry has a distinctive power to distinguish the natural populations like various ore grades within a deposit.

These fractal methods proved their superiority to the classical statistical and conventional geological methods which are used commonly. The reasons of their superiority to other methods are as follows (Agterberg et al. 1993; Cheng et al. 1994; Sim et al. 1999):

1. In classical statistics, for the purpose of determining the boundaries in mineralized zones, frequency distribution of a related element in an intended area must adhere to normal distribution. This requirement is not always met so the data must be normalized.

2. Those values which are not within the range (outliers) must be identified and eliminated accordingly; otherwise they lead to the intended study having unreal results.

3. Spatial distribution of the samples is important in classical statistics which means that all samples are considered independently and this is not reasonable.

4. The geometrical shape of anomalies does not receive attention in any other way, so that the area covered by each specific grade is not significant.

Concentration-volume (C-V) fractal model

The C-V fractal model, which was proposed by Afzal et al. (2011) for division of mineralized zones and barren host rocks in porphyry deposits, can be addressed as:

$$V(\rho \leq \upsilon) \propto \rho^{-a1}\ ; V(\rho \geq \upsilon) \propto \rho^{-a2} \quad (1)$$

Where $V(\rho \leq \upsilon)$ and $V(\rho \geq \upsilon)$ illustrate two volumes with concentration values less than or equal to and greater than or equal to the contour value ρ; υ indicates the threshold value of a mineralized zone (or volume); and a1 and a2 are characteristic exponents. Elemental threshold values in this model represent boundaries between different mineralized zones and host rocks of mineral deposits. To calculate $V(\rho \leq \upsilon)$ and $V(\rho \geq \upsilon)$, which are the volumes enclosed by a contour level ρ in a 3D block model, the borehole data of ore element concentrations were interpolated by utilization of geostatistical estimation.

The selection of breakpoints as threshold values appears to be an objective decision because geochemical populations are defined by different line segments in the C-V log-log plot. The straight fitted lines were obtained based on least-square regression (Agterberg et al. 1996; Spalla et al. 2010). In other words, the intensity of element enrichment is depicted by each slope of the line segment in the C-V log-log plots.

The C-V fractal model is applied for separating enrichment zones, especially the supergene enrichment zone from the hypogene zone and wall rocks using the concentration values of the zones in combination with characteristic features of their geometrical shapes such as ore veins. The C-V model is applicable to ore elements in porphyry deposits such as Cu and Mo for which the spatial patterns of concentration values satisfy a multifractal model (Daneshvar et al. 2012).

Geological setting of Kahang deposit

The Kahang deposit of about 20 km^2 is located about 73 km NE of Isfahan in Central Iran. This deposit contains more than 80 million tonnes of sulphide ore with an average grade of 0.5 % Cu and 90 ppm Mo according to the latest exploration results. The deposit is situated in the Cenozoic Urumieh-Dokhtar magmatic belt of the Zagros orogen extending from NW to SE Iran depicted in Fig. 1 (Stocklin 1977; Berberian & King 1981; Alavi 1994; Dargahi et al. 2010). The Iranian large Cu-Mo-Au porphyry deposits such as Sarcheshmeh, Sungun, Meiduk and Darehzar are located on the belt (Shahabpour 1994). The Kahang Cu-Mo porphyry deposit was explored by remote sensing, geophysical methods and drilling operations which are being carried out in a detailed exploration stage (Tabatabaei & Asadi Haroni 2006; Afzal et al. 2010, 2012).

This deposit is mainly composed of Eocene volcanic-pyroclastic rocks, which were intruded by quartz monzonite, monzogranite-diorite to dioritic intrusions in Oligo-Miocene rocks (Fig. 1). The extrusive rocks, including tuffs, breccias and lavas are dacitic to andesitic composition.

On the other hand, these intrusions are roots of acidic to intermediate domes in the Kahang porphyry deposit. The main structural features are two fault systems trending NE-SW and NW-SE. The major alteration zones of potassic, phyllic, argillic and propylitic types were accompanied by vein to veinlets fillings of quartz, quartz-magnetite and Fe-hydroxides. Mineralization within intrusive bodies and their surrounding host rocks consists of chalcocite, chalcopyrite, pyrite, malachite, magnetite, limonite jarosite, goethite and chalcantite in quartz stockworks and advanced argillic alteration. The eastern part of the deposit is covered by phyllic and quartz-sericite alteration (Rashidnejad Omran et al. 2011).

According to descriptive models (Cox & Singer 1986), copper ores existing in the supergene zone consist of two ore minerals such as covellite (CuS) and chalcocite (Cu_2S) which contain 65 % to 80 % of copper. Bornite is found in this zone

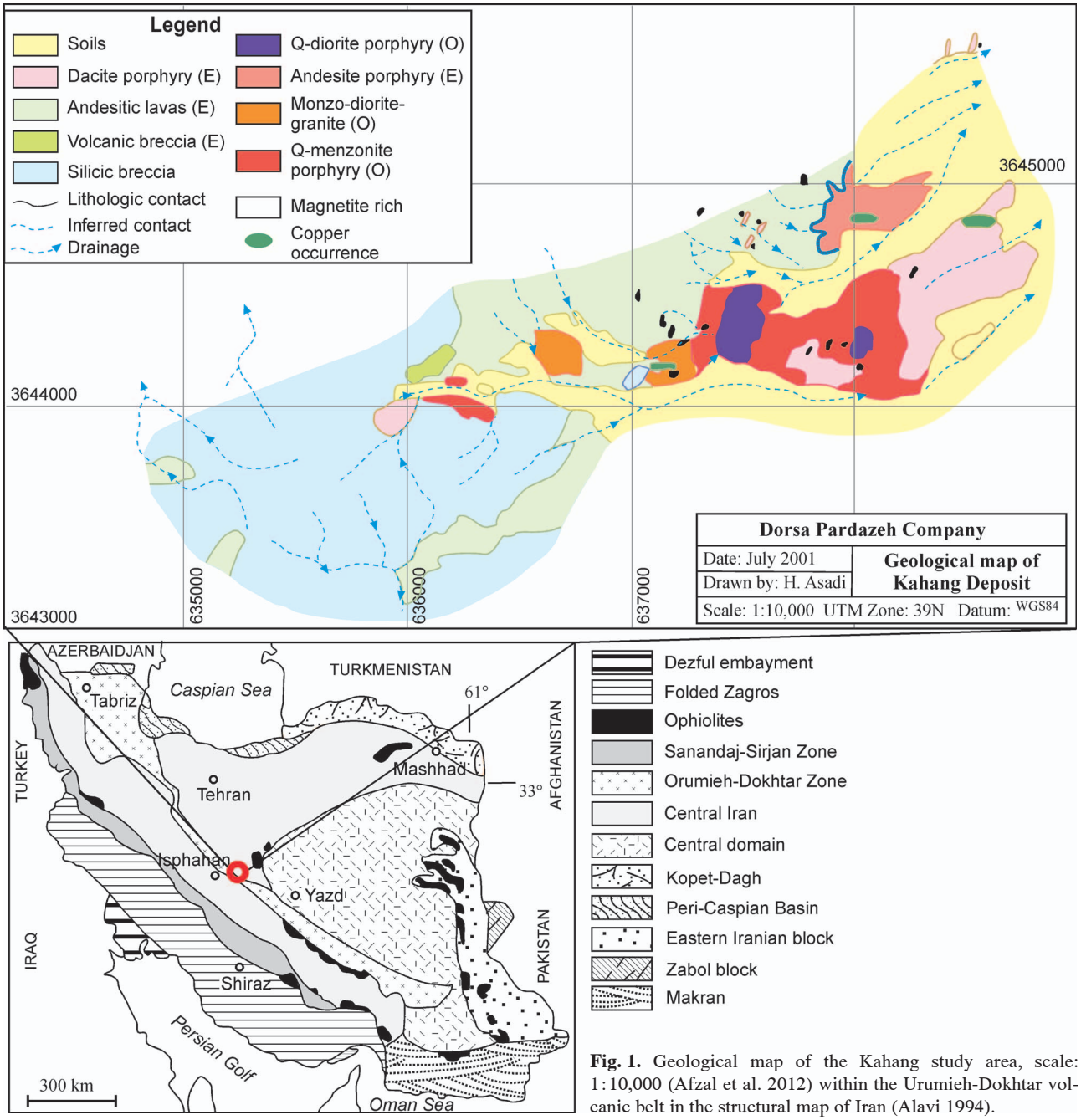

Fig. 1. Geological map of the Kahang study area, scale: 1:10,000 (Afzal et al. 2012) within the Urumieh-Dokhtar volcanic belt in the structural map of Iran (Alavi 1994).

but the amount of chalcopyrite is low. In the hypogene zone, the amounts of chalcocite and covellite are decreased while chalcopyrite and then bornite are considered as the main minerals. Potassic alteration consists of orthoclase (Kf) and biotite which occur in the central parts of porphyry deposits, according to the model of Lowell & Guilbert (1970). Phyllic is the main alteration in mineralized parts of the porphyry deposits which include quartz, muscovite, sericite and chlorite.

Geological 3D models

The 3D geological models have been generated from lithological, mineralogical and alteration data recorded in 48 boreholes using RockWorks™ v. 15 software. The subsurface data include coordinates of drillcores, azimuth and dip (orientation), lithology, alteration, mineralography and zonation. The project dimensions are 600×660×780 m in X, Y and Z direction and each voxel has a dimension of 4×4×10 m respectively.

Major rock types in the deposit are sub-volcanic acidic units such as andesitic, trachytic, dacitic and dioritic rocks, as depicted in Fig. 2. Andesitic and trachytic units surround other rock types in this deposit. Dacitic rocks contain ores in the SE part of the area of this study which concludes that Dacitic units are the host rock of the SE part in the deposit. The most frequent host rock is porphyric quartz-diorite including Cu-Mo ore accumulation which is the index of subvolcanic acidic rocks (Fig. 2).

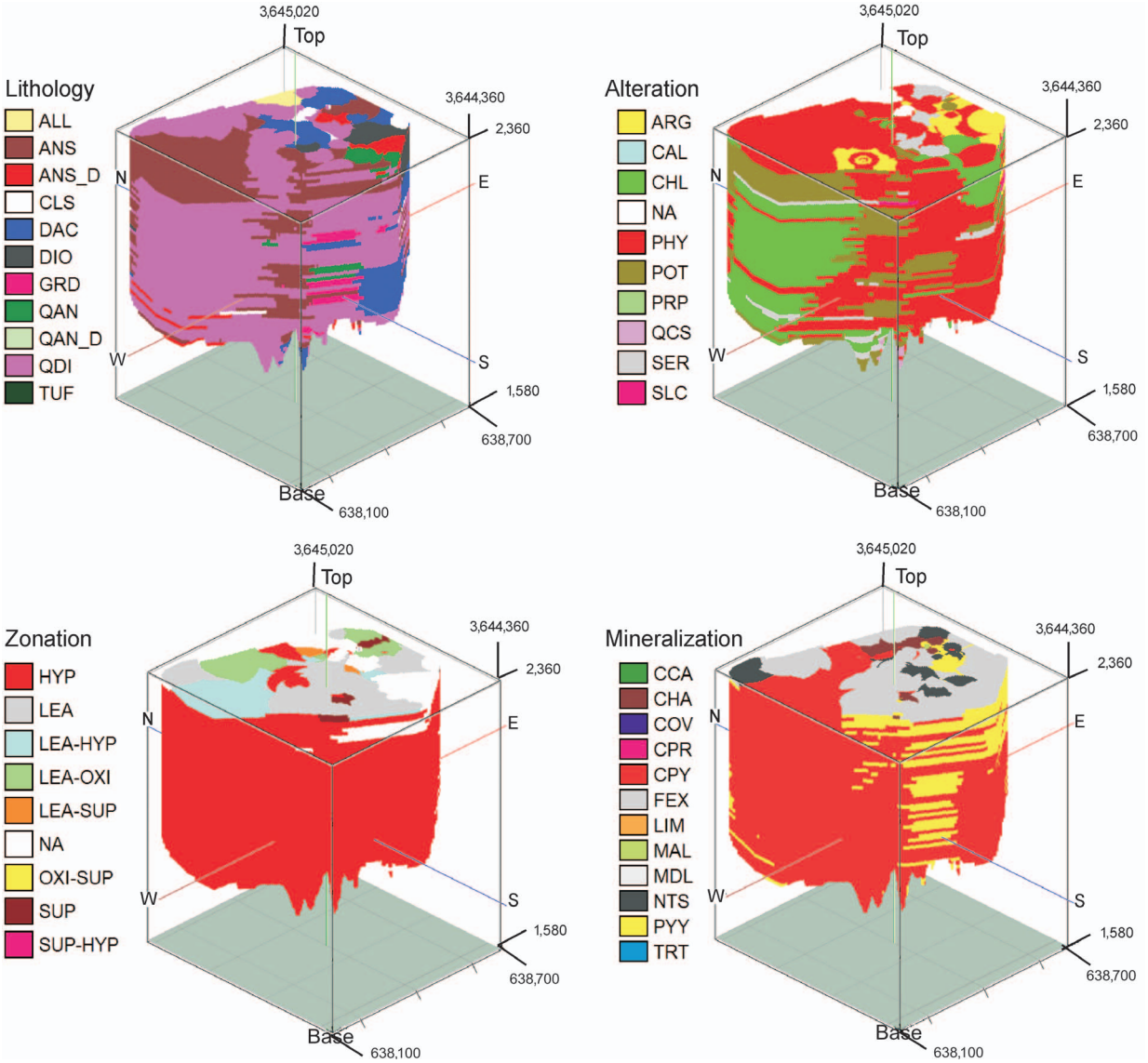

Fig. 2. Geological 3D models including lithology, alteration, zonation and mineralization with the legend of each in the Kahang Cu-Mo porphyry deposit. Abbreviations see in Appendix. (Scale is in m^3.)

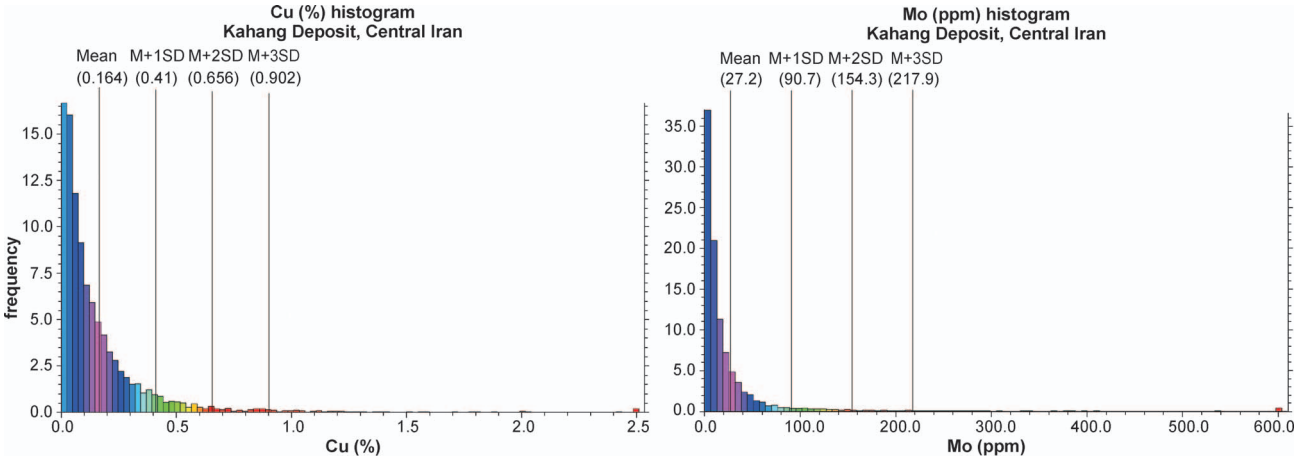

Fig. 3. Cu and Mo histograms in the Kahang deposit.

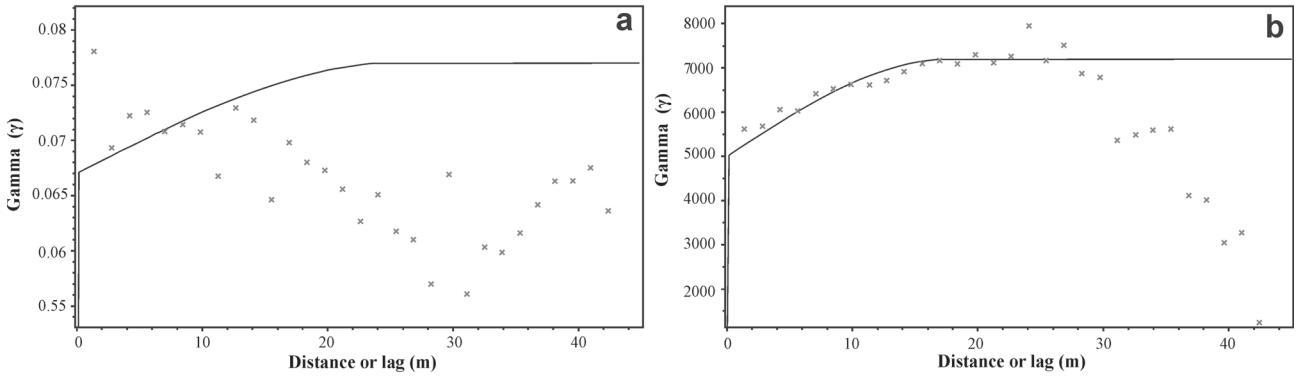

Fig. 4. Experimental variograms for Cu (**a**) and Mo (**b**).

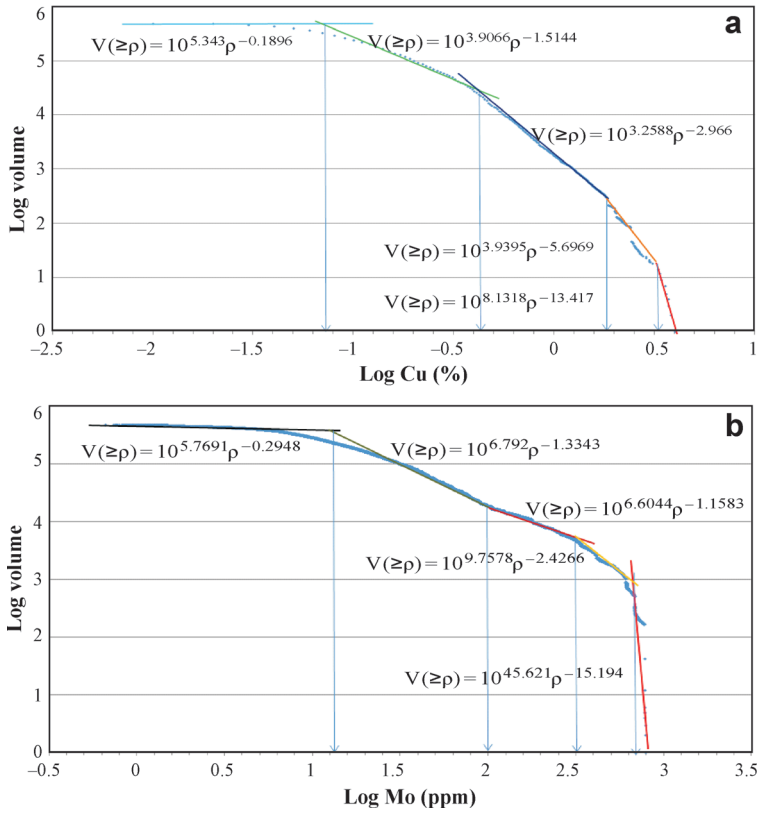

Fig. 5. C-V log-log plots for Cu (**a**) and Mo (**b**).

Phyllic is the most frequent alteration in the Kahang deposit in terms of its size and expansion as illustrated in Fig. 2. Potassic alteration is situated at depth and deepens as it goes to the east part of the deposit although potassic alteration exists near the surface in the west part of this porphyry deposit. Other alterations namely argillic and propylitic are small and occur near the surface as illustrated in Fig. 2.

Studies related to zonation in this deposit represent that the most significant ore mineralization zone is hypogene in terms of size and high percentage of chalcopyrite which can be easily seen in the 3D model illustrated in Fig. 2. The supergene enrichment zone and chalcocite are limited with thicknesses of less than 10 m in the eastern part of the deposit. Chalcocite accumulation is situated in the central part of the area, as illustrated in Fig. 2. Fe-oxides are seen at the surface and in the oxidation zone (Fig. 2). Additionally, pyrite as a fundamentally important index of a copper porphyry deposit is present in several parts of the deposit, and malachite ore is very low with regards to volume in the oxidized zone.

C-V fractal modelling

In this deposit, 7146 samples were collected from 48 boreholes at 2 m intervals. The samples were analysed by the ICP-MS method for Cu and Mo concentrations. The Cu and Mo distribution functions are not normal, with Cu and Mo averages of 0.166 % and 28 ppm, respectively (Fig. 3). The experimental variograms for Cu and Mo were calculated by SGeMS software as shown in Fig. 4 and their ranges are 24 and 17 m for Cu and Mo respectively. Experimental variograms of Cu and Mo, specifically Cu, in the deposit indicate "hole effects" which shows there are different mineralized zones and ore-forming processes (Journel & Froidevaux 1982). The Kahang deposit was modelled with 489,927 voxels and each voxel had a dimension of 4×4×10 m in the X, Y and Z directions based on the geometrical properties of the deposit and grid drilling dimensions (David 1970). 3D models of the distribution for Cu and Mo were evaluated by Ordinary Kriging (OK) using SGeMS and RockWorks software. Ordinary Kriging is a spatial evaluation technique where the error variance is minimized which is called the Kriging variance. It is based on the configuration of the data and on the variogram (Yamamoto 2000).

The C-V fractal model for Cu has been created according to the Cu 3D block model. It reveals that there are 5 populations according to the log-log plot corresponding to 0.075 %, 0.42 %, 1.86 % and 3.24 % in this deposit (Fig. 5 and Table 1). The first threshold of 0.075 % represents the beginning of the Cu mineralization in this scenario. As a result of this, the range of Cu concentrations less than 0.075 % is

Table 1: Cu and Mo thresholds defined by C-V model in the Kahang deposit.

Geochemical population	Cu (%) threshold value	Mo (ppm) threshold value	Range Cu (%)	Range Mo (ppm)
First (Barren host rock)	–	–	<0.075	<13
Second (Main mineralization starting)	0.075	13	0.075–0.42	13–100
Third	0.42	100	0.42–1.86	100–316
Fourth	1.86 (Enriched zone for Cu)	316	1.86–3.24	316–645
Fifth	3.24	645 (Enriched zone for Mo)	>3.24	>645

deemed as barren host rock. The second threshold value of Cu is 0.42 % where the main Cu mineralization starts. The range of Cu concentrations higher than 1.86 % illustrates an enriched zone for Cu. For these Cu concentrations the slope of the straight line fit is near to 90°.

Based on the 3D model of Mo distribution, volumes corresponding to different Mo grades were considered to generate a C-V fractal model. Threshold values of Mo were identified in the C-V log-log plot which reveals five geochemical populations and four threshold values equal to 13, 100, 316 and 645 ppm (Fig. 5 and Table 1). Enriched mineralized zones are deemed to have higher than 645 ppm because with these Mo concentrations the slope of the straight line fit is close to 90°. The main Mo mineralization starts from the second threshold which is 100 ppm in this kind of scenario. It is important to bear in mind that the Mo concentration greater than 13 ppm represents the start of Mo mineralization so therefore any amount less than 13 ppm is considered as barren host rock in terms of Mo distribution. Cu and Mo log-log plots have a multifractal nature for the elemental mineralization in the deposit.

Comparison and correlation of C-V with geological models

To separate major mineralized zones including the supergene enrichment and hypogene zones, a correlation of the geological model (as mentioned in section 4) with Cu and Mo concentration distribution models has been constructed and in addition results from the C-V model were applied on the combined model where in consequence the supergene enrichment zone exists in small parts close to the surface and its Cu concentration value does not exceed by 1.4 % (Fig. 6). The various mineralized zones were distinguished by a mathematical filter facility of RockWorks software which is called "Boolean data

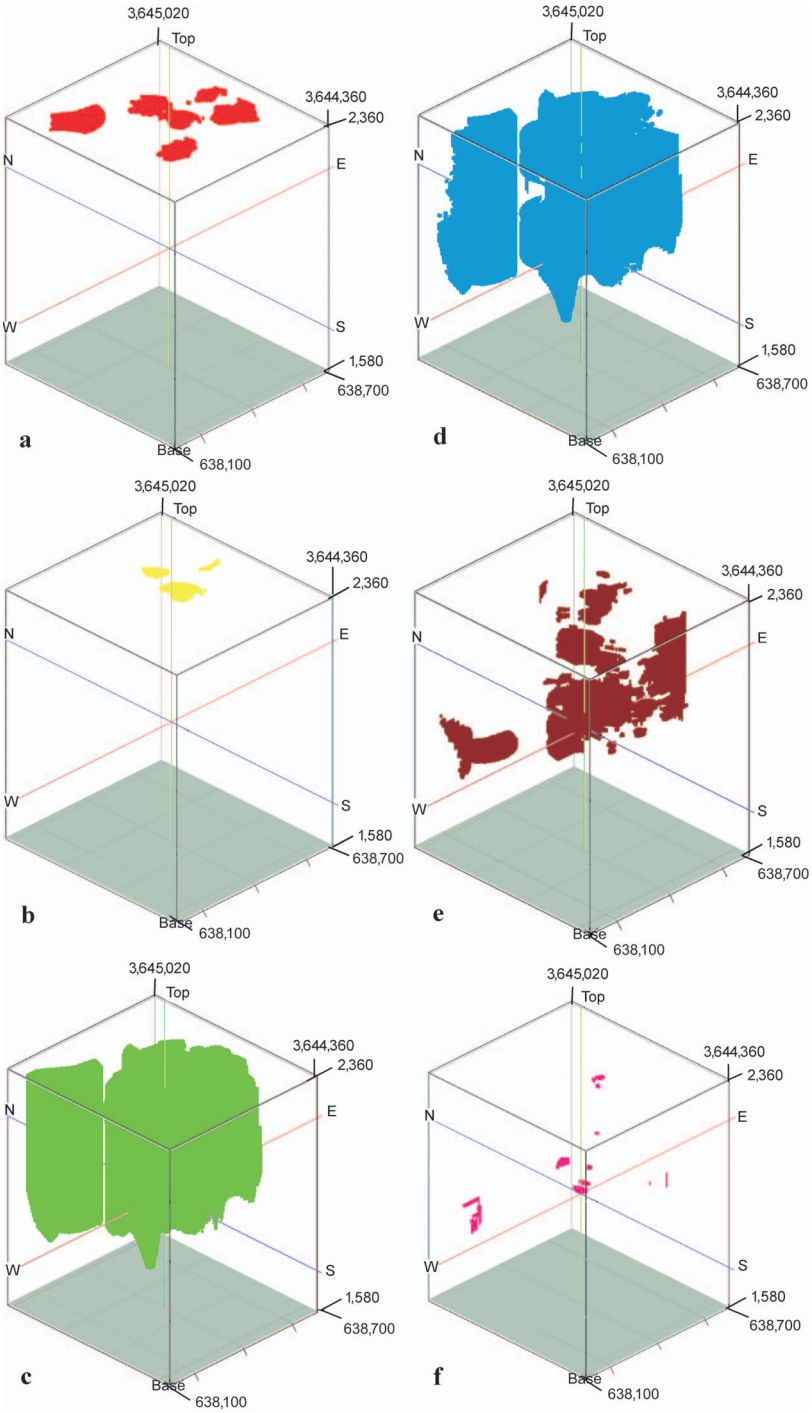

Fig. 6. Geological zones (Cu distribution) including supergene enrichment (**a**) and hypogene (**c**) with modified zonation models via C-V containing of supergene enrichment (**b**), hypogene (**d**), main hypogene (**e**) and enriched hypogene (**f**). (Scale is in m^3.)

type". As a result, the studied mineralized zones in the 3D model are allocated with binary codes (zero or one) which represent that the zones with the code number of zero are removed and the zones with the code number of one will remain in the 3D model.

The supergene enrichment zone with 0.42 < Cu concentrations (starting main Cu mineralization based on C-V model) is located in small areas within the central and eastern parts of the deposit, as depicted in Fig. 6b, as can be seen, the supergene enrichment zone derived via the C-V model has a volume smaller than its geological equivalent model.

The correlation between the geological hypogene zone and the C-V model indicate that marginal parts of the geological model have Cu concentration ≤0.075 % and is consequently not considered as a hypogene mineralized zone. However, the main hypogene zone with Cu≥0.42 % is located in the central, eastern and NW parts of the deposit especially at depth, but in the NE part of the deposit it approaches the surface. The enriched hypogene zone with Cu≥1.8 % is situated in small parts of the central, NW, NE and SE of the deposit, as illustrated in Fig. 6.

The Mo distribution model is correlated with the supergene enrichment and the hypogene zones, as depicted in Fig. 7. The maximum concentration of Mo in the supergene enrichment zone is 104 ppm and high values of Mo are situated in the hypogene zone. The main Mo mineralization with Mo≥100 ppm in the hypogene zone correlates with the main hypogene zone (Cu≥0.42 %). The enriched Mo zone with Mo≥645 ppm is located in the central part of the deposit and associated with the enriched hypogene zone (Cu≥1.8 %), as shown in Fig. 7. These outcomes indicate that the enriched mineralized zone is located within the hypogene zone especially in the central, NW and NE parts of the deposit.

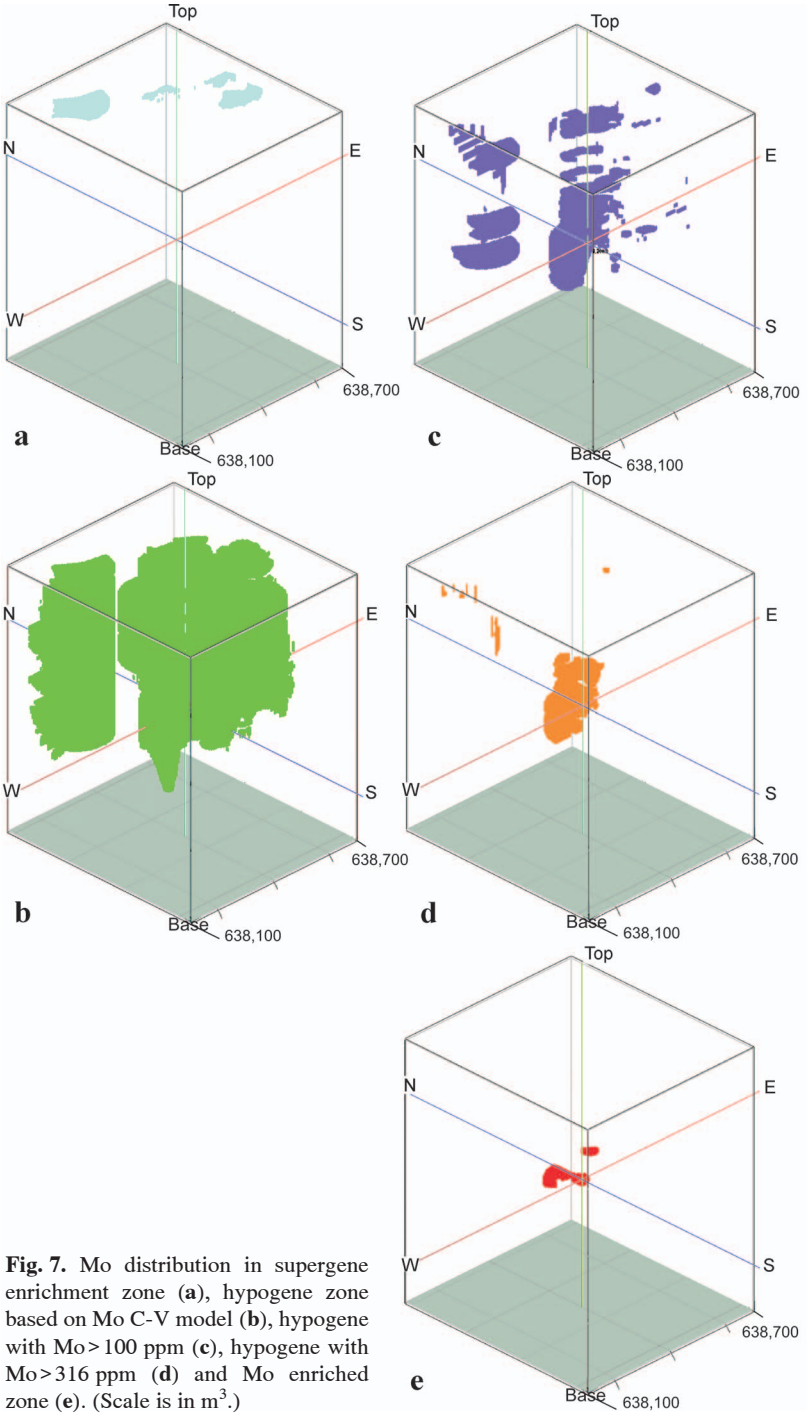

Fig. 7. Mo distribution in supergene enrichment zone (**a**), hypogene zone based on Mo C-V model (**b**), hypogene with Mo > 100 ppm (**c**), hypogene with Mo > 316 ppm (**d**) and Mo enriched zone (**e**). (Scale is in m^3.)

In order to validate the accuracy of the C-V model, a correlation between the mineralography model (for chalcocite and chalcopyrite distributions) and the mineralized zones was carried out by C-V model which showed that chalcocite is associated with the supergene enrichment zone and chalcopyrite is also located in the hypogene zone (Fig. 8). In addition, the chalcopyrite model with Cu≥0.42 % has a strong correlation with the main hypogene zone, as depicted in Fig. 8e.

Application of logratio matrix

Carranza (2011) has proposed a logratio matrix to analyse further calculation of spatial correlations between two binary models. Using the mineralization model, an intersection operation between a fractal mineralized zone model and different zones in geological ore model was performed to obtain numbers of voxels corresponding to each of the four classes of overlap zones as shown in the Table 2. Using the obtained numbers of voxels, Type I error (T1E), Type II error (T2E), and overall accuracy (denoted as OA) relates to the ability of the analysis to barren host rocks (background) and mineralized zones of the fractal models were estimated with respect to the geological ore model. Type I error (denoted as T1E) relates to the ability of the analysis to barren host rocks

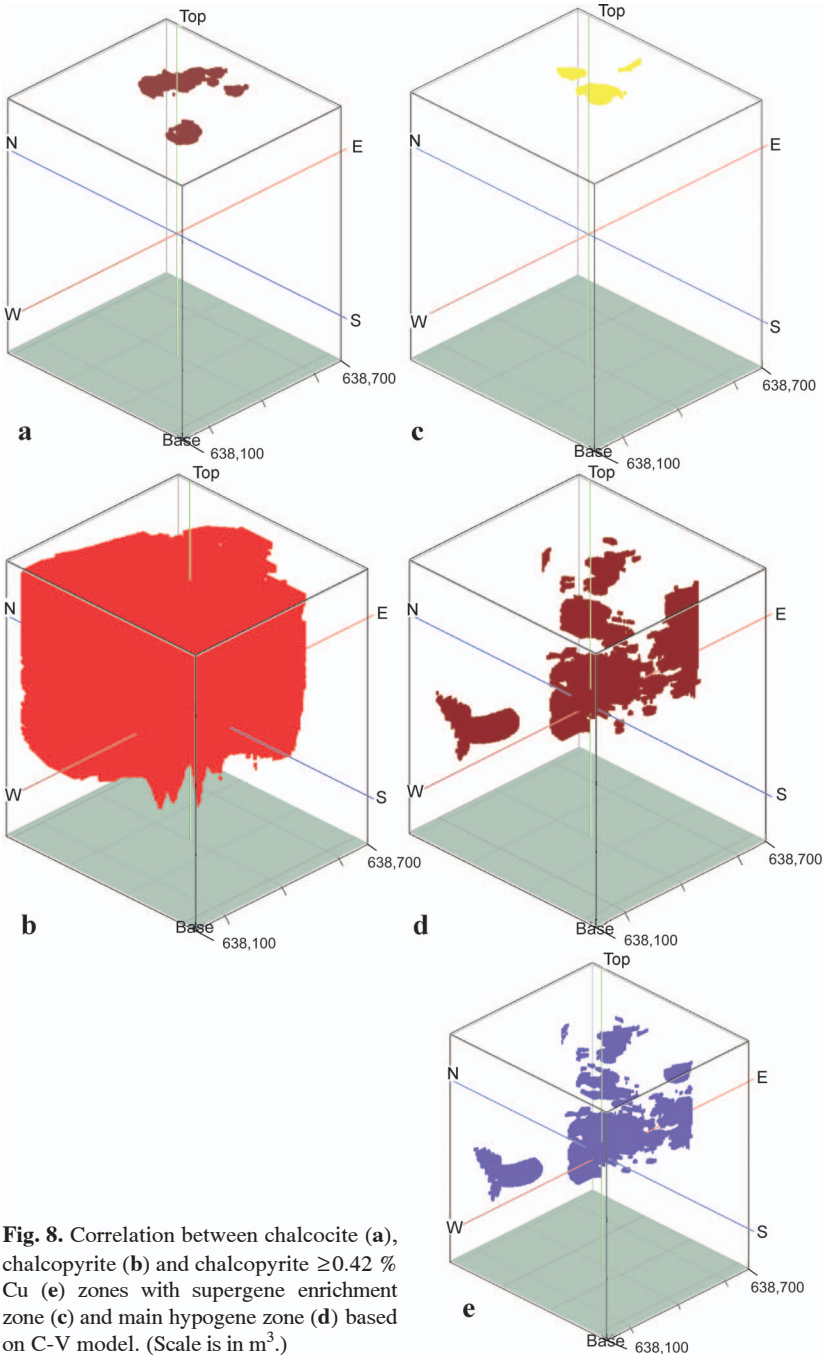

Fig. 8. Correlation between chalcocite (**a**), chalcopyrite (**b**) and chalcopyrite ≥0.42 % Cu (**e**) zones with supergene enrichment zone (**c**) and main hypogene zone (**d**) based on C-V model. (Scale is in m^3.)

whereas Type II error (denoted as T2E) relates to the ability of the analysis to mineralized zones. The lower both errors (i.e. the higher value for OA) are the better ability of the analysis meanwhile to barren host rocks and mineralized zones. The values for OA of C-V fractal and geological models (alteration and hypogene models) were compared with one another as follows.

Comparison between the hypogene zone obtained from the geological model and the main Cu and Mo mineralized zones from C-V fractal model demonstrates that the hypogene zone has better correlation with the main Cu mineralized zone (Cu > 0.42%) because the number of overlapping voxels (A) in the main Cu mineralized zone obtained by C-V model (20,839 voxels) is higher than in the main Mo mineralized zone (16,990 voxels), as depicted in Table 3. The overall accuracy of the main Cu and Mo mineralized zone derived via the C-V fractal model with respect to the hypogene zone of the geological model is equal to 0.154 and 0.146 respectively.

Alterations play a fundamental role in zone identification and also in presenting geological models, as described by Lowell & Guilbert (1970). Correlation (from OA results) between the main Cu mineralized zone obtained from C-V model and potassic alteration is higher than phyllic alteration because the OA for potassic and phyllic alterations have been determined as 0.765 and 0.509 respectively (Table 4). As a result, the higher values for overall accuracy in Tables 3 and 4 represent the higher overlap between geological zones with mineralized zones identified by the C-V fractal model.

Validation between the main Mo mineralized zone (Mo > 100 ppm) based on the C-V fractal model and alteration zones from the geological model indicates that there is a difference between the two alteration zones. Overall accuracy for the potassic and phyllic zones has been determined as 0.770 and 0.524 respectively (Table 5). According to these results, the main elemental mineralized zones have better correlation with the potassic alteration zone.

Conclusion

The results from this study reveal that the hypogene zone is a major mineralized zone within the Kahang Cu-Mo porphyry deposit. According to the C-V fractal model, the main threshold values for Cu and Mo are 0.42 % and 100 ppm, respectively. Enriched Cu-Mo mineralized zones with Cu ≥ 1.8 % and Mo ≥ 645 ppm are located in the central, NW and NE parts within the hypogene zone. The supergene enrichment zone exists in small parts within the deposit, especially in the central and eastern parts.

The supergene enrichment and hypogene zones delineated by the C-V model correlate well with the alterations and mineralogical data shown in the 3D models. The C-V log-log plots from the Kahang deposit show that there is a multifractal model for Cu and Mo. Correlation between the results of the C-V model and the chosen geological particulars show that the supergene enrichment zone has a high correlation within the chalcocite accumulations within the Kahang de-

Table 2: Matrix for comparing performance of fractal modelling results with geological model. A, B, C, and D represent numbers of voxels in overlaps between classes in the binary geological model and the binary results of fractal models (Carranza 2011).

		Geological model	
		Inside zone	**Outside zone**
Fractal model	**Inside zone**	True positive (A)	False positive (B)
	Outside zone	False negative (C)	True negative (D)
		Type I error = C/(A+C)	Type II error = B/(B+D)
		Overall accuracy = (A+D)/(A+B+C+D)	

Table 3: Overall accuracy (OA) with respect to the hypogene zone resulted from the geological model and main Cu and Mo mineralized zones obtained through the C-V fractal model.

		Hypogene zone of Geological model			
		Inside zone		**Outside zone**	
C-V fractal model of Cu main mineralized zone	**Inside zone**	A	20,839	B	3,348
	Outside zone	C	411,164	D	54,576
		OA		0.154	
		Hypogene zone of Geological model			
		Inside zone		**Outside zone**	
C-V fractal model of Mo main mineralized zone	**Inside zone**	A	16,990	B	1,795
	Outside zone	C	414,954	D	54,674
		OA		0.146	

Table 4: Overall accuracy (OA) with respect to potassic and phyllic alteration zones and main Cu mineralized zones obtained through the C-V fractal model.

		Potassic alteration zone of Geological model			
		Inside zone		**Outside zone**	
C-V fractal model of Cu main mineralized zone	**Inside zone**	A	2,874	B	21,313
	Outside zone	C	93,484	D	372,256
		OA		0.765	
		Phyllic alteration zone of Geological model			
		Inside zone		**Outside zone**	
C-V fractal model of Cu main mineralized zone	**Inside zone**	A	10,345	B	13,842
	Outside zone	C	226,246	D	239,494
		OA		0.509	

Table 5: Overall accuracy (OA) with respect to potassic and phyllic alteration zones and main Mo mineralized zones obtained through the C-V fractal model.

		Potassic alteration zone of Geological model			
		Inside zone		**Outside zone**	
C-V fractal model of Mo main mineralized zone	**Inside zone**	A	1,699	B	17,086
	Outside zone	C	95,053	D	374,575
		OA		0.770	
		Phyllic alteration zone of Geological model			
		Inside zone		**Outside zone**	
C-V fractal model of Mo main mineralized zone	**Inside zone**	A	11,531	B	7,254
	Outside zone	C	224,919	D	244,709
		OA		0.524	

posit. The main hypogene zone has an association with the chalcopyrite distribution model having Cu≥0.42 %. According to the correlation between results driven by fractal modelling and geological models by logratio matrix, the main Cu and Mo mineralized zones generated by the C-V fractal model have a strong correlation with the potassic alteration zone with respect to overall accuracy.

Acknowledgments: The authors are grateful to the National Iranian Copper Industries Co. (NICICO) for their permission to have access to the Kahang deposit dataset. Additionally, the authors would like to thank Dr. A. Saad Mohammadi the former CEO of NICICO for his support. The authors would like to thank the reviewers of this paper for their comments and valuable remarks.

References

Afzal P., Khakzad A., Moarefvand P., Rashidnejad Omran N., Esfandiari B. & Fadakar Alghalandis Y. 2010: Geochemical anomaly separation by multifractal modelling in Kahang (Gor Gor) porphyry system, Central Iran. *J. Geochem. Exploration* 104, 34–46.

Afzal P., Fadakar Alghalandis Y., Khakzad A., Moarefvand P. & Rashidnejad Omran N. 2011: Delineation of mineralization zones in porphyry Cu deposits by fractal concentration-volume modeling. *J. Geochem. Exploration* 108, 220–232.

Afzal P., Fadakar Alghalandis Y., Khakzad A., Moarefvand P., Rashidnejad Omran N. & Asadi Haroni H. 2012: Application of power-spectrum-volume fractal method for detecting hypogene, supergene enrichment, leached and barren zones in Kahang Cu porphyry deposit, Central Iran. *J. Geochem. Exploration* 112, 131–138.

Agterberg F.P., Cheng Q. & Wright D.F. 1993: Fractal modeling of mineral deposits. In: Elbrond J. & Tang X. (Eds.): 24th APCOM Symposium Proceeding. Montreal, Canada, 43–53.

Agterberg F.P., Cheng Q., Brown A. & Good D. 1996: Multifractal modeling of fractures in the Lac du Bonnet Batholith, Manitoba. *Computers and Geosciences* 22, 497–507.

Alavi M. 1994: Tectonic of Zagros orogenic belt of Iran: new data and interpretations. *Tectonophysics* 229, 211–238.

Ali Kh., Cheng Q. & Zhijun C. 2007: Multifractal power spectrum and singularity analysis for modelling stream sediment geochemical distribution patterns to identify anomalies related to gold mineralization in Yunnan Province, South China. *Geochemistry: Exploration, Environment, Analysis* 7, 4, 293–301.

Asghari O. & Hezarkhani A. 2008: Appling discriminant analysis to separate the alteration zones within the Sungun porphyry copper deposit. *Asian J. Applied Sci*. 8, 24, 4472–4486.

Beane R.E. 1982: Hydrothermal alteration in silicate rocks. In: Titley S.R. (Ed.): Advances in geology of the porphyry copper deposits, Southwestern North America. *The University of Arizona Press*, Tucson, 117–137.

Berberian M. & King G.C. 1981: Towards a paleogeography and tectonic evolution of Iran. *Canad. J. Earth Sci*. 18, 210–265.

Berger B.R., Ayuso R.A., Wynn J.C. & Seal R.R. 2008: Preliminary model of porphyry copper deposits. *USGS, Open-File Report*, 1–1321.

Carranza E.J.M. 2008: Geochemical anomaly and mineral prospectivity mapping in GIS. Handbook of exploration and environmental geochemistry. Vol. 11. *Elsevier*, Amsterdam, 1–351.

Carranza E.J.M. 2009: Controls on mineral deposit occurrence inferred from analysis of their spatial pattern and spatial association with geological features. *Ore Geol. Rev*. 35, 383–400.

Carranza E.J.M. 2011: Analysis and mapping of geochemical anomalies using logratio-transformed stream sediment data with censored values. *J. Geochem. Exploration* 110, 167–185.

Carranza E.J.M. & Sadeghi M. 2010: Predictive mapping of prospectively and quantitative estimation of undiscovered VMS deposits in Skellefte district (Sweden). *Ore Geol. Rev*. 38, 219–241.

Carranza E.J.M., Owusu E. & Hale M. 2009: Mapping of prospectivity and estimation of number of undiscovered prospects for lode-gold, southwestern Ashanti Belt, Ghana. *Mineralium Depos*. 44, 8, 915–938.

Cheng Q. 1999: Spatial and scaling modelling for geochemical anomaly separation. *J. Geochem. Exploration* 65, 3, 175–194.

Cheng Q. 2007: Mapping singularities with stream sediment geochemical data for prediction of undiscovered mineral deposits in Gejiu, Yunnan Province, China. *Ore Geol. Rev*. 32, 314–324.

Cheng Q. & Agterberg F.P. 2009: Singularity analysis of ore-mineral and toxic trace elements in stream sediments. *Computers and Geosciences* 35, 2, 234–244.

Cheng Q., Agterberg F.P. & Ballantyne S.B. 1994: The separation of geochemical anomalies from background by fractal methods. *J. Geochem. Exploration* 51, 109–130.

Cox D. & Singer D. 1986: Mineral deposits models. *U.S. Geol. Surv. Bull*., 1–1693.

Daneshvar Saein L., Rasa I., Rashidnejad Omran N., Moarefvand P. & Afzal P. 2012: Application of concentration-volume fractal method in induced polarization and resistivity data interpretation for Cu-Mo porphyry deposits exploration, case study: Nowchun Cu-Mo deposit, SE Iran. *Nonlinear Processes in Geophysics* 19, 431–438.

Dargahi S., Arvin M., Pan Y. & Babaei A. 2010: Petrogenesis of post-collisional A-type granitoids from the Urumieh–Dokhtar magmatic assemblage, Southwestern Kerman, Iran: Constraints on the Arabian–Eurasian continental collision. *Lithos* 115, 190–204.

David M. 1977: Geostatistical ore reserve estimation. *Elsevier*, Amsterdam, 1–283.

Goncalves M.A., Mateus A. & Oliveira V. 2001: Geochemical anomaly separation by multifractal modeling. *J. Geochem. Exploration* 72, 91–114.

Journel A.G. & Froidevaux R. 1982: Anisotropic hole-effect modelling. *Mathematical Geol*. 14, 217–239.

Lauwerier H. 1991: Fractals: Images of chaos. *Princeton University Press*, New Jersey, 1–240.

Li C., Ma T. & Shi J. 2003: Application of a fractal method relating concentrations and distances for separation of geochemical anomalies from background. *J. Geochem. Exploration* 77, 167–175.

Lima A., De Vivo B., Cicchella D., Cortini M. & Albanese S. 2003: Multifractal IDW interpolation and fractal filtering method in environmental studies: an application on regional stream sediments of (Italy), Campania region. *Applied Geochem*. 18, 1853–1865.

Lowell J.D. 1968: Geology of the Kalamazoo orebody, San Manuel district, Arizona. *Economic Geol*. 63, 645–654.

Lowell J.D. & Guilbert J.M. 1970: Lateral and vertical alteration-mineralization zoning in porphyry ore deposits. *Economic Geol*. 65, 373–408.

Lucido G., Caponetti E. & Triolo R. 1991: Fractality as a working tool for petrology: small-angle neutron scattering experiments to detect critical behaviour of magma. *Geol. Carpathica* 42, 85–91.

Mandelbrot B.B. 1983: The fractal geometry of nature. *W.H. Freeman*, San Fransisco, 1–468.

Melfos V., Vavelidis M., Christo des G. & Seidel E. 2002: Origin and evolution of the Tertiary Maronia porphyry copper-molybdenum deposit, Thrace, Greece. *Mineralium Depos*. 37, 648–668.

Nash J.T. 1976: Fluid inclusion petrology-data from porphyry copper deposits and applications to exploration. *U.S. Geol. Surv. Prof. Pap*., Vol. 907-D, 1–16.

Ortega O.J., Marrett R. & Laubach S.E. 2006: A scale-independent approach to fracture intensity and average fracture spacing. *Amer. Assoc. Petrol. Geol. Bull*. 90, 2, 193–208.

Rashidnejad Omran N., Afzal P., Harati H., Moarefvand P., Asadi Haroni H. & Daneshvar Saeein L. 2011: Application of power-law frequency fractal model in determination of vertical geochemical distribution of Cu in Kahang porphyry deposit, Central Iran. *J. Mining and Metallurgy* 47A, 1, 1–8.

Roedder E. 1971: Fluid inclusion studies on the porphyry-type ore deposits at Bingham, Utah, Butte, Montana, and Climax, Colorado. *Econ. Geol*. 66, 98–120.

Schwartz G.M. 1947: Hydrothermal alteration in the "porphyry copper" deposits. *Econ. Geol*. 42, 319–352.

Shahabpour J. 1994: Post-mineral breccia dyke from the Sar-Cheshmeh porphyry copper deposit, Kerman, Iran. *Explor. and Mining Geol*. 3, 39–43.

Shen W. & Zhao P. 2002: Theoretical study of statistical fractal model with applications to mineral resource prediction. *Computers and Geosciences* 28, 369–376.

Sillitoe R.H. 1997: Characteristics and controls of the largest porphyry copper-gold and epithermal gold deposits in the circum-Pacific region. *Australian J. Earth Sci*. 44, 373–388.

Sim B.L., Agterberg F.P. & Beaudry C. 1999: Determining the cut off between background and relative base metal contamination levels using multifractal methods. *Computers and Geosciences* 25, 1023–1041.

Spalla M.I., Morotta A.M. & Gosso G. 2010: Advances in interpretation of geological processes: refinement of multi-scale data and integration in numerical modelling. *Geol. Soc. London*, 1–240.

Stocklin J.O. 1977: Structural correlation of the Alpine ranges between Iran and Central Asia. *Mem. Hors Service Soc. Geol. France* 8, 333–353.

Tabatabaei S.H. & Asadi Haroni H. 2006: Geochemical characteristics of Gor Gor Cu-Mo porphyry system. *25th Iranian Symposium on Geosciences, Geological Survey of Iran*, 1–60.

Takayasu H. 1990: Fractals in the physical sciences. *Manchester University Press*, Manchester and New York, 1–176.

Turcotte D.L. 1986: A fractal approach to the relationship between ore grade and tonnage. *Econ. Geol*. 18, 1525–1532.

Ulrich T., Gunther D. & Heinrich C.A. 2001: The evolution of a porphyry Cu–Au deposit, based on La-ICP-MS analysis of fluid inclusions, Bajo de la Alumbrera, Argentina. *Econ. Geol*. 96, 1743–1774.

Wang Q.F., Deng J., Liu H., Wang Y., Sun X. & Wan L. 2011: Fractal models for estimating local reserves with different mineralization qualities and spatial variations. *J. Geochem. Exploration* 108, 196–208.

Wilson A.J., Cooke David R., Harper B.J. & Deyell C.L. 2007: Sulfur isotopic zonation in the Cadia district, southeastern Australia: exploration significance and implications for the genesis of alkalic porphyry gold-copper deposits. *Mineralium Depos*. 42, 465–487.

Yamamoto J.K. 2000: An alternative measure of the reliability of Ordinary Kriging Estimates. *Mathematical Geology* 32, 489–507.

Zuo R. 2011: Decomposing of mixed pattern of arsenic using fractal model in Gangdese belt, Tibet, China. *Applied Geochem*. 26, 271–273.

Zou R., Cheng Q. & Xia Q. 2009: Application of fractal models to characterization of vertical distribution of geochemical element concentration. *J. Geochem. Exploration* 102, 1, 37–43.

Appendix

Full names of all abbreviations in the manuscript content.

Lithology	ALL	ALLUVIUM	**Alteration**	ARG	ARGILLIC
	ANS	ANDESITE		CAL	CALCITIZED
	ANS–D	ANDESITE–DIORITE		CHL	CHLORITIC
	CLS	CORE LOSS		NA	Not Available
	DAC	DACITE		PHY	PHYLLIC
	DIO	DIORITE		POT	POTASSIC
	GRD	GRANODIORITE		PRP	PROPYLITIC
	QAN	QUARTZ ANDESITE		QCS	QUARTZ–CHLORITE–SERICITE
	QAN–D	QUARTZ ANDESITE–DIORITE		SER	SERICITIC
	QDI	QUARTZ DIORITE		SLC	SILCIFIC (SILICIC)
	TUF	TUFF			
Zonation	HYP	HYPOGENE	**Mineralization**	CCA	CHRYSOCOLLA
	LEA	LEACHED		CHA	CHALCOCITE
	LEA–HYP	LEACHED–HYPOGENE		COV	COVELLITE
	LEA–OXI	LEACHED–OXIDE		CPR	CUPRITE
	LEA–SUP	LEACHED–SUPERGENE		CPY	CHALCOPYRITE
	NA	Not Available		FEX	IRON OXIDE
	OXI–SUP	OXIDE–SUPERGENE		LIM	LIMONITE
	SUP–HYP	SUPERGENE–HYPOGENE		MAL	MALACHITE
				MDL	MOLYBDENITE
				NTS	NEOTOCITE
				PYY	PYRITE
				TRT	TENORITE